Dynamics of Sharma-Mittal holographic dark energy model in Brans-Dicke theory of gravity

Y. Aditya[1,*], U.Y. Divya Prasanthi[2]
[1] Department of Mathematics, GMR Institute of Technology, Rajam-532127, India
[2] Department of Statistics and Mathematics, College of Horticulture, Dr. Y.S.R. Horticultural University, Parvathipuram-535501, India
aditya.y@gmrit.edu.in
(Submitted on 14.06.2022; Accepted on 07.07.2022)

Abstract. The Sharma-Mittal holographic dark energy is studied in this research work using the Brans-Dicke scalar-tensor theory of gravity with a background of spatially homogeneous and anisotropic Kantowski-Sachs space-time. We use the Brans-Dicke scalar field $\phi(t)$ as a function of the average scale factor $a(t)$ in this case. The physical behaviour of the model is addressed using a graphical depiction to investigate the universe's accelerating expansion. Furthermore, the models' stability is tested using squared sound speed v_s^2. For our models, the well-known cosmic plane $\omega_{de} - \omega'_{de}$ is constructed. It is also worth noting that the conclusions of deceleration, equations of state parameters, and the $\omega_{de} - \omega'_{de}$ and statefinder planes are all consistent with modern observational evidence.
Key words: Kantowski-Sachs model, Holographic dark energy, Scalar field, Scalar-tensor theory.

Introduction

Recent observational evidence on the history of cosmic expansion (Perlmutter et al. 1999; Riess et al. 1998) has led to the discovery of accelerating universe expansion. The cause is thought to be dark energy (DE), an exotic sort of unknown force with extremely high negative pressure. The nature and behaviour of DE, on the other hand, remain a mystery. There are two major approaches to dealing with the problem of cosmic acceleration: either introducing a dark energy component into the Universe and studying its dynamics (Caldwell 2002; Sahni and Starobinsky 2000; Padmanabhan 2008; Sharif and Zubair 2010; Santhi et al. 2016a, 2017a), or interpreting it as a failure of general relativity and considering modifying Einstein's theory of gravitation.

Among the different dynamical DE models, the holographic dark energy (HDE) model, in particular, has been a prominent tool for studying the DE mystery in recent years. It was based on quantum properties of black holes (BH), which have been widely studied in the literature to research quantum gravity (Li 2004; Susskind 1995). Leading to the generation of BH in quantum field theory, the holographic principle states that the bound on the vacuum energy Λ of a system with size L should not cross the limit of the BH mass of the same size. The energy density of HDE is defined as follows (Cohen et al. 1999):

$$\rho_{de} = 3d^2 m_p^2 L^{-2}, \tag{1}$$

where the reduced Planck mass is m_p, the numerical constant is $3d^2$, and the IR-cutoff is L. Several IR-cutoffs such as the Hubble horizon H^{-1}, the event horizon, the particle horizon, the conformal universe age, the Ricci scalar radius, and the Granda–Oliveros cutoff have all been explored in the literature (Gao et al. 2006; Wei and Cai 2008). These HDE models with varied IR-cutoffs

can provide a recent scenario of universe acceleration and also demonstrate that the value of the transition redshift from early deceleration ($q > 0$) to current acceleration ($q < 0$) is consistent with modern observational data. It can also help with the problem of cosmic coincidence (why the energy densities due to the dark matter and the DE should have a constant ratio for the present universe). Various studies have shown that the HDE model agrees fairly well with the observational data (Xu and Wang 2010; Duran and Pavon 2011). Nojiri and Odintsov (2006) presented a method for uniting the universe's early and late epochs based on generalised HDE and phantom cosmology, while Hinflation (Nojiri et al. 2019) recently generalised the same concept. In a Dvali-Gabadadze-Porrati (DGP) braneworld, Ghaffari (2019) investigated the cosmological dynamics of HDE. Tanisman (2019) investigated the HDE model and found that the generalised rules of thermodynamics for the D-dimensional Kaluza-Klein-type Friedmann-Robertson-Walker (FRW) universe are true. Various cosmological aspects of new and modified HDE models have been investigated by a number of researchers (Reddy et al. 2016; Aditya and Reddy 2018; Rao et al. 2018; Santhi et al. 2017a, 2017b; Naidu et al. 2018).

Several entropy formalisms have been used to construct and study cosmological models in recent years. Tsallis HDE (Tavayef et al. 2018; Tsallis and Cirto 2013), Sharma-Mittal HDE (Jahromi et al. 2018), and Renyi HDE model (Moradpour et al. 2018) are some of the new HDE models that have been developed. Tsallis HDE, based on Tsallis generalised entropy, is never stable at the classical level, whereas Sharma-Mittal HDE is classically stable in the situation of non-interacting cosmos. Renyi HDE is predicated on the absence of interconnections across cosmic sectors, and it is more stable on its own (Moradpour et al. 2018). In a flat FRW universe with Chern-Simons modified gravity, Younas et al. (2019) have investigated Tsallis, Renyi, and Sharma-Mittal entropies. In logarithmic Brans–Dicke theory, Aditya et al. (2019a) examined observational constraints on Tsallis HDE. Prasanthi and Aditya (2020, 2021) have studied observational constraints in Renyi HDE. Tsallis, Renyi, and Sharma-Mittal HDE models in the D-dimensional fractal universe were discussed by Maity and Debnath (2019). Iqbal and Jawad (2019) explored three HDE models in a flat FRW universe within the DGP braneworld, whereas Jawad et al. (2018) examined three HDE models in loop quantum cosmology. Sharma and Dubey (2020) have explored the Sharma-Mittal HDE models with several diagnostic tools. As a result of the foregoing studies, we consider the HDE with new entropy formalism, i.e., Sharma-Mittal HDE with Hubble horizon as IR cutoffs in this work.

Some large-angle anomalies (Eriksen et al. 2004) are discovered in cosmic microwave background radiations, which contradict the universe's statistical isotropy. In cosmological models, the cosmos may have acquired a small anisotropic geometry regardless of inflation. Many researchers have recently investigated numerous cosmological models with anisotropic backgrounds using modified theories of gravitation (Sharif and Shamir 2010; Rao et al. 2015a, 2015b, 2015c; Santhi et al. 2015, 2017c, 2018, 2019; Aditya et al. 2016). In this study, we explore Kantowski-Sachs universe in the presence of pressureless matter and Sharma-Mittal HDE within the context of Brans-Dicke theory of gravity (Brans and Dicke 1961). The paper is structured as follows: The derivation of field equations and solutions of field equations are covered in

Sect. 1. The model's physical properties are discussed in Sect. 2. The last section contains a summary and conclusions.

1. Field equations and the model

We consider the Kantowski-Sachs space-time in the following form

$$ds^2 = dt^2 - A^2 dr^2 - B^2(d\psi^2 + sin^2\psi d\varphi^2), \tag{2}$$

where A and B are only cosmic time t functions. Anisotropic and homogeneous yet expanding (or contracting) cosmologies are described by the Kantowski-Sachs class of metrics. They also provide models for estimating and comparing the consequences of anisotropies with the FRW class of cosmologies (Thorne 1967).

As alternatives to Einstein's general theory of relativity, various gravitational theories have been proposed. However, the scalar-tensor theory developed by Brans and Dicke (1961) is regarded as the best alternative to Einstein's theory. We suppose a universe filled with pressure-less matter with an energy density of ρ_m and dark energy with a density of ρ_{de}. As a result, the Brans-Dicke field equations for the combined scalar and tensor fields are given in this case by

$$R_{ij} - \frac{1}{2}Rg_{ij} = -\frac{8\pi}{\phi}(T_{ij} + \overline{T}_{ij}) - \phi^{-1}\left(\phi_{i;j} - g_{ij}\phi^{;\alpha}_{;\alpha}\right) - w\phi^{-2}\left(\phi_{,i}\phi_{,j} - \frac{1}{2}g_{ij}\phi_{,\alpha}\phi^{,\alpha}\right), \tag{3}$$

$$\phi^{;\alpha}_{;\alpha} = \frac{8\pi}{(3+2w)}(T + \overline{T}) \tag{4}$$

and the energy conservation equation is

$$(T_{ij} + \overline{T}_{ij})_{;j} = 0, \tag{5}$$

which is the result of field equations (3) and (4). In this case, R is a Ricci scalar, R_{ij} is a Ricci tensor, and w is a dimensionless coupling constant. T_{ij} and $\overline{T}_{ij}$ are energy-momentum tensors for pressure-less matter and Sharma-Mittal HDE, which are defined as

$$T_{ij} = \rho_m u_i u_j; \qquad \overline{T}_{ij} = (\rho_{de} + p_{de})u_i u_j - p_{de}g_{ij} \tag{6}$$

here p_{de} and ρ_{de} are the pressure and energy density of DE, respectively, and ρ_m is energy density of matter. The equation of state (EoS) (ω_{de}) parameter of DE is defined as $\omega_{de} = \frac{p_{de}}{\rho_{de}}$.

The field equations (3) for the metric (2) produce the following equations when adopting co-moving coordinates:

$$2\frac{\ddot{B}}{B}+\frac{\dot{B}^2}{B^2}+\frac{1}{B^2}+\frac{w}{2}\frac{\dot{\phi}^2}{\phi^2}+\frac{\ddot{\phi}}{\phi}+2\frac{\dot{B}\dot{\phi}}{B\phi}=-\frac{\omega_{de}\rho_{de}}{\phi} \tag{7}$$

$$\frac{\ddot{A}}{A}+\frac{\ddot{B}}{B}+\frac{\dot{A}\dot{B}}{AB}+\frac{w}{2}\frac{\dot{\phi}^2}{\phi^2}+\frac{\ddot{\phi}}{\phi}+\frac{\dot{\phi}}{\phi}\left(\frac{\dot{A}}{A}+\frac{\dot{B}}{B}\right)=-\frac{\omega_{de}\rho_{de}}{\phi} \tag{8}$$

$$2\frac{\dot{A}\dot{B}}{AB}+\frac{\dot{B}^2}{B^2}+\frac{1}{B^2}-\frac{w}{2}\frac{\dot{\phi}^2}{\phi^2}+\frac{\dot{\phi}}{\phi}\left(\frac{\dot{A}}{A}+2\frac{\dot{B}}{B}\right)=\frac{\rho_m+\rho_{de}}{\phi} \tag{9}$$

$$\ddot{\phi}+\dot{\phi}\left(\frac{\dot{A}}{A}+2\frac{\dot{B}}{B}\right)=\frac{(\rho_{de}-3p_{de}+\rho_m)}{\phi(3+2w)}, \tag{10}$$

and the conservation equation is given by

$$\dot{\rho_m}+\dot{\rho_{de}}+\left(\frac{\dot{A}}{A}+2\frac{\dot{B}}{B}\right)(\rho_m+(1+\omega_{de})\rho_{de})=0, \tag{11}$$

where the overhead dot represents ordinary differentiation with respect to cosmic time t.

For the Kantowski-Sachs model, we define the main parameters:
Hubble's parameter of the model

$$H=\frac{\dot{a}}{a}, \tag{12}$$

where

$$a(t)=(AB^2)^{1/3} \tag{13}$$

is the average scale factor. The anisotropic parameter A_h is given by

$$A_h=\frac{1}{3}\sum_{i=1}^{3}\left(\frac{H_i-H}{H}\right)^2, \tag{14}$$

where $H_1=\frac{\dot{A}}{A}, H_2=H_3=\frac{\dot{B}}{B}$ are directional Hubble's parameters, which express the expansion rates of the universe in the directions of r, ψ and φ, respectively.
Expansion scalar and shear scalar are defined as

$$\theta=u^i_{;i}=\frac{\dot{A}}{A}+2\frac{\dot{B}}{B} \tag{15}$$

$$\sigma^2=\frac{1}{2}\sigma^{ij}\sigma_{ij}=\frac{1}{3}\left(\frac{\dot{A}}{A}-\frac{\dot{B}}{B}\right)^2, \tag{16}$$

where σ_{ij} is shear tensor, A_h is the deviation from isotropic expansion and the universe expands isotropically if $A_h = 0$. Deceleration parameter is given by

$$q = \frac{d}{dt}\left(\frac{1}{H}\right) - 1. \tag{17}$$

If $-1 \leq q < 0$, the universe expands at an accelerating rate, decelerating volumetric expansion occurs if $q > 0$. If $q = 0$, the universe expands at a constant rate.

$A(t)$, $B(t)$, $\phi(t)$, ω_{de}, ρ_{de}, and ρ_m are six unknown variables in the four equations (7)-(10). As a result, some extra constraints are required to solve the above system of equations. We build our computations on the following physically acceptable assumptions:

(i). The shear scalar (σ) is assumed to be proportional to the expansion scalar (θ). This results in a relationship between the metric potentials (Collins et al. 1980), i.e.,

$$A = B^k, \tag{18}$$

where $k \neq 1$ is a constant that accounts for space-time anisotropy. The physical foundation for this assumption can be found in observations of the velocity-redshift relation for extragalactic sources, which indicates that the Hubble expansion of the universe may achieve isotropy when $\frac{\sigma}{\theta}$ is constant (Kantowski and Sachs 1966).

(ii). In addition, it is common in the literature to employ a power-law relationship between the scalar field ϕ and the average scale factor $a(t)$ of the form $\phi \propto [a\,(t)]^n$ (Johri and Sudharsan 1989; Johri and Desikan 1994) where n denotes a power index. Many authors have looked into different aspects of this type of scalar field ϕ (Santhi et al. 2016b, 2017d; Naidu et al. 2020, 2021; Raju et al. 2019, 2020a; Aditya et al. 2019b, 2020, 2021, 2022; Dasunaidu et al. 2021; Bhaskara Rao et al. 2021, 2022). Given the physical significance of preceding relationship i.e., $\phi \propto [a\,(t)]^n$, we employ the following assumption to reduce the mathematical complexity of the system:

$$\phi(t) = \phi_0[a(t)]^n. \tag{19}$$

From Eqs. (7), (8), (18) and (19), we obtain the metric potentials as

$$A = \left(\frac{t^2}{k-1} - c_1\ (k-1)\right)^{\frac{k}{2}} \tag{20}$$

$$B = \sqrt{\frac{t^2}{k-1} - c_1\ (k-1)}, \tag{21}$$

where c_1 is an integrating constant and $n(k+2) + 3k = 0$. Now, the scalar field ϕ calculated as

$$\phi(t) = \phi_0\ \left(\frac{t^2}{k-1} - c_1\ (k-1)\right)^{\frac{1}{6\,n(k+2)}}. \tag{22}$$

Consequently, the metric (2) can be rewritten as

$$ds^2 = dt^2 - \left(\frac{t^2}{k-1} - c_1\ (k-1)\right)^k dr^2 - \left(\frac{t^2}{k-1} - c_1\ (k-1)\right)(d\psi^2 + sin^2\psi d\varphi^2). \tag{23}$$

2. Cosmological parameters and Discussion

Equation (23), together with Eq. (22), demonstrates the Kantowski-Sachs universe with Sharma-Mittal HDE in Brans-Dicke theory of gravity. The physical and geometrical parameters listed below are critical in the discussion of cosmology.
The spatial volume (V) and the average scale factor ($a(t)$) of the model are given by

$$V(t) = [a(t)]^3 = \left(\frac{t^2}{k-1} - c_1\ (k-1)\right)^{\frac{k+2}{2}}. \tag{24}$$

The mean Hubble's parameter (H) and the expansion scalar (θ) are obtained as

$$H = \frac{\theta}{3} = \frac{(k+2)\,t}{3\,t^2 - 3\,c_1\ (k-1)^2}. \tag{25}$$

The shear scalar (σ^2) and the anisotropic parameter (A_h) are

$$\sigma^2 = \frac{(k-1)^2\,t^2}{3\left(t^2 - \ c_1\ (k-1)^2\right)^2}, \tag{26}$$

$$A_h = \frac{2(k-1)^2}{(k+2)^2}. \tag{27}$$

Eq. (23) denotes the spatially homogeneous and anisotropic Kantowski - Sachs Sharma-Mittal HDE cosmological model in the Brans-Dicke theory of gravity. Our model is free of initial singularity, i.e. at $t = 0$. From a finite volume when $t = 0$, the model's spatial volume increases with time. This demonstrates that the model has expanded spatially. At $t = 0$, the parameters $H(t)$, $\theta(t)$, and σ^2 are finite and disappear as $t \to \infty$. The mean anisotropic parameter A_h represents the deviation from isotropic expansion. It determines whether the model is isotropic or anisotropic. When $k = 1$, $A_h = 0$. The universe expands isotropically in this particular case. In addition, if $V \to \infty$ and $A_h = 0$ as $t \to \infty$, the model approaches isotropy continuously.

As a dynamical dark energy component, we assume Sharma-Mittal holographic dark energy. It is formulated using Sharma-two-parametric Mittal's entropy (Sharma and Mittal 1975)

$$S_{SM} = \frac{1}{d_1}\left(\left(1 + \frac{\delta\kappa}{4}\right)^{\frac{d_1}{\delta}} - 1\right), \tag{28}$$

where $\kappa = 4\pi L^2$ and L represents the IR cutoff. d_1 and δ are two free parameters in this case. At the appropriate d_1 limits, Renyi and Tsallis entropies can be recovered. Sharma-Mittal entropy is transformed into Renyi entropy in the limit $d_1 \to 0$, and Tsallis entropy in the limit $d_1 \to 1-\delta$. According to Cohen et al. (1999), the relationship between the system entropy and the IR and UV cutoffs yields the energy density

$$\rho_{de} = \frac{3d_2^2 S_{SM}}{8\pi L^4}. \tag{29}$$

Using the above equation and the Hubble horizon cutoff $L = \frac{1}{H}$, we can calculate the energy density of the Sharma-Mittal HDE model (Jahromi et al. 2018) as follows:

$$\rho_{de} = \frac{3d_2^2 H^4}{8\pi d_1}\left(\left(1+\frac{\delta\pi}{H^2}\right)^{\frac{d_1}{\delta}} - 1\right), \tag{30}$$

where d_2^2 denotes the free parameter. The above equation can be written using Eq. (25) as

$$\rho_{de} = \frac{d_2^2\left((k+2)\,t\right)^4}{27\left(t^2 - c_1\ (k-1)^2\right)^4 d_1}\left(\left(1+\frac{9\delta\pi(t^2-c_1(k-1)^2)^2}{\left((k+2)\,t\right)^2}\right)^{\frac{d_1}{\delta}} - 1\right) \tag{31}$$

Using Eqs. (20)-(22) and (31) in Eqs. (7)-(9), we get the energy density of matter and EoS parameter as

$$\begin{aligned}\rho_m(t) = \phi_0\ &\left(\frac{t^2}{k-1} - c_1\ (k-1)\right)^{\frac{1}{6\,n(k+2)}}\left\{\frac{2kt^2}{\left(t^2 - c_1\ (k-1)^2\right)^2} + \frac{t^2}{\left(t^2 - c_1\ (k-1)^2\right)^2}\right.\\ &+\left(\frac{t^2}{k-1} - c_1\ (k-1)\right)^{-1} - \frac{wn^2\,(k+2)^2\,t^2}{2\left(3\,t^2 - 3\,c_1\ (k-1)^2\right)^2} + \frac{n\,(k+2)\,t}{3\,t^2 - 3\,c_1\ (k-1)^2}\\ &\left.\times\left(\frac{kt}{t^2 - c_1\ (k-1)^2} + 2\,\frac{t}{t^2 - c_1\ (k-1)^2}\right)\right\} - \frac{d_2^2\left((k+2)\,t\right)^4}{27\left(t^2 - c_1\ (k-1)^2\right)^4 d_1}\\ &\times\left(\left(1+\frac{9\delta\pi(t^2-c_1(k-1)^2)^2}{\left((k+2)\,t\right)^2}\right)^{\frac{d_1}{\delta}} - 1\right)\end{aligned} \tag{32}$$

$$\omega_{de}(t) = \left\{ \frac{-3c_1\ (k-1)^2}{\left(t^2 - c_1\ (k-1)^2\right)^2} + \frac{k\,(k-1)\left(t^2 - c_1\ (k-1)\right)}{\left(t^2 - c_1\ (k-1)^2\right)^2} \right.$$
$$+ \frac{t^2}{\left(t^2 - c_1\ (k-1)^2\right)^2} + \frac{kt^2}{\left(t^2 - c_1\ (k-1)^2\right)^2} + \frac{wn^2\,(k+2)^2\,t^2}{\left(3\,t^2 - 3\,c_1\ (k-1)^2\right)^2}$$
$$+ \frac{2n\,(k+2)\left(n\,(k+2)\,t^2 - 3\,t^2 - 3\,c_1\ (k-1)^2\right)}{9\left(t^2 - c_1\ (k-1)^2\right)^2} + \frac{n\,(k+2)\,t}{3\,t^2 - 3\,c_1\ (k-1)^2}$$
$$\times \left\{ \frac{kt}{t^2 - c_1\ (k-1)^2} + 3\,\frac{t}{t^2 - c_1\ (k-1)^2} \right\} + \left(\frac{t^2}{k-1} - c_1\ (k-1) \right)^{-1} \Bigg\}$$
$$\times \frac{\phi_0\ \left(\frac{t^2}{k-1} - c_1\ (k-1) \right)^{\frac{1}{6\,n(k+2)}}}{\frac{d_2^2((k+2)t)^4}{27\left(t^2 - c_1\ (k-1)^2\right)^4 d_1} \left(\left(1 + \frac{9\delta\pi(t^2 - c_1(k-1)^2)^2}{((k+2)t)^2} \right)^{\frac{d_1}{\delta}} - 1 \right)} \tag{33}$$

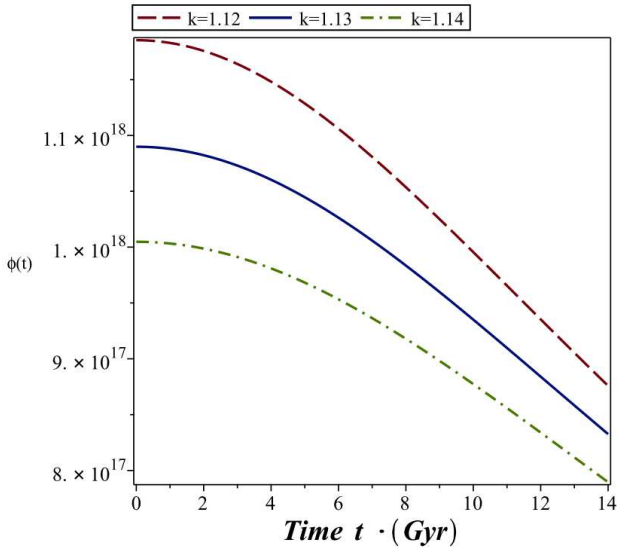

Fig. 1. Plot of the scalar field ϕ versus cosmic time t for $\phi_0 = 9 \times 10^{19}$, and $c_1 = -19000$.

Scalar field: We plotted the behaviour of scalar field versus cosmic time for various values of the parameter k in Fig. 1. The scalar field can be seen to be a positive and decreasing function that eventually approaches a minimum positive value. The scalar field exhibits decreasing behaviour, and thus, the corresponding kinetic energy increases. This behaviour is very similar to the

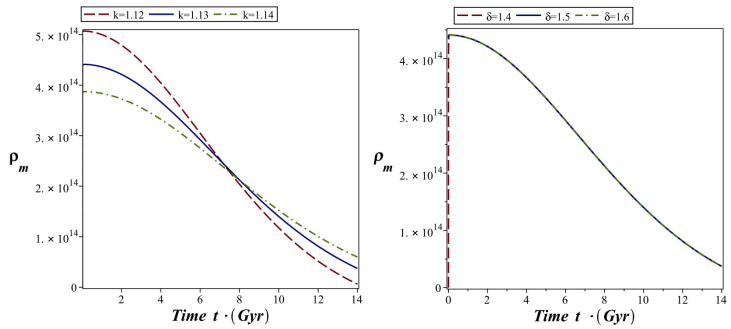

Fig. 2. Plot of the energy density ρ_m versus cosmic time t for $\phi_0 = 9 \times 10^{19}$, $c_1 = -19000$, $w = 0.008$, $d_2 = 2.2$ and $d_1 = 4.5$.

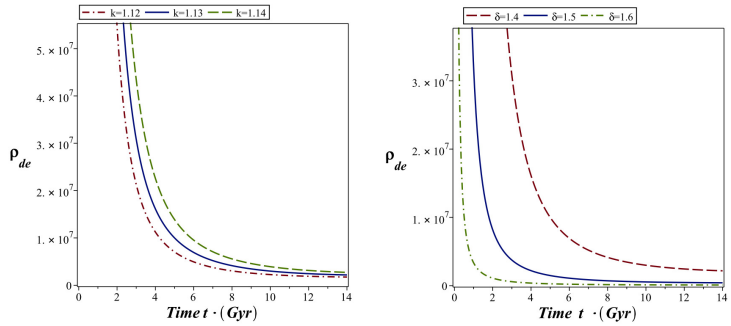

Fig. 3. Plot of the energy density ρ_{de} versus cosmic time t for $c_1 = -19000$, $d_2 = 2.2$ and $d_1 = 4.5$.

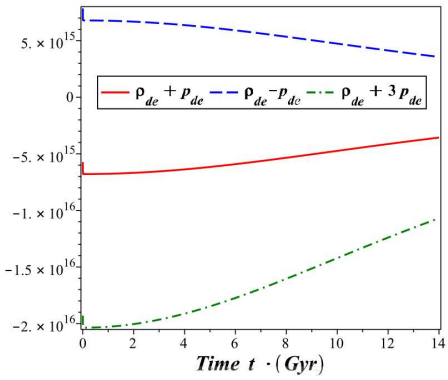

Fig. 4. Plot of the energy conditions versus cosmic time t for $\phi_0 = 9 \times 10^{19}$, $c_1 = -19000$, $\delta = 1.5$, $w = 0.008$, $d_2 = 2.2$, $d_1 = 4.5$, and $k = 1.13$.

behaviour of scalar fields in dark energy models constructed by several authors in the literature (Jawad et al. 2015; Aditya and Reddy 2019; Naidu et al. 2019).

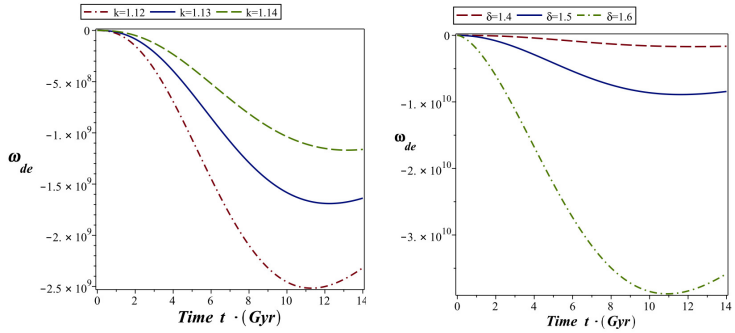

Fig. 5. Plot of the EoS parameter ω_{de} versus cosmic time t for $\phi_0 = 9 \times 10^{19}$, $c_1 = -19000$, $w = 0.008$, $d_2 = 2.2$ and $d_1 = 4.5$.

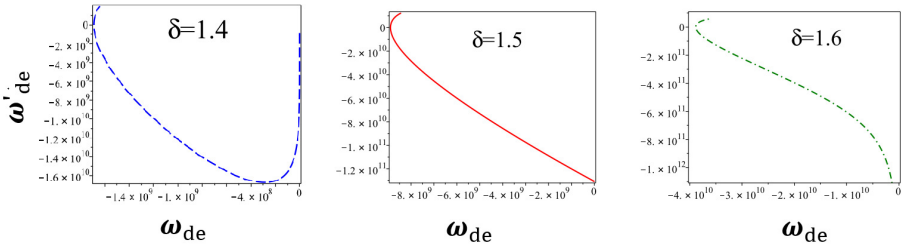

Fig. 6. Plot of the $\omega_{de} - \omega'_{de}$ plane for $\phi_0 = 9 \times 10^{19}$, $c_1 = -19000$, $w = 0.008$, $d_2 = 2.2$, $d_1 = 4.5$, and $k = 1.13$.

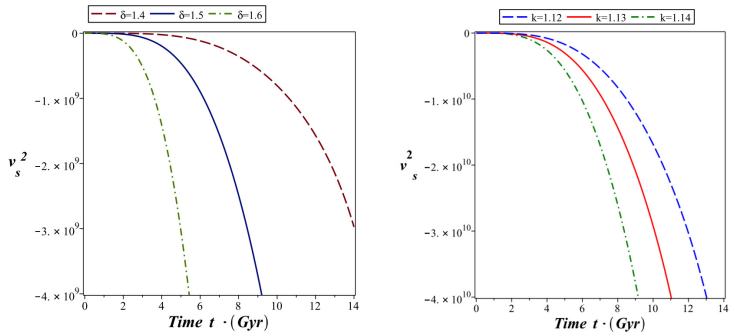

Fig. 7. Plot of the squared sound speed v_s^2 versus cosmic time t for $\phi_0 = 9 \times 10^{19}$, $c_1 = -19000$, $w = 0.008$, $d_2 = 2.2$ and $d_1 = 4.5$.

It can also be seen that the scalar field decreases as the parameter k increases. Hence, in this work, we would like to study the other dynamical parameters in the light of Brans-Dicke scalar field.

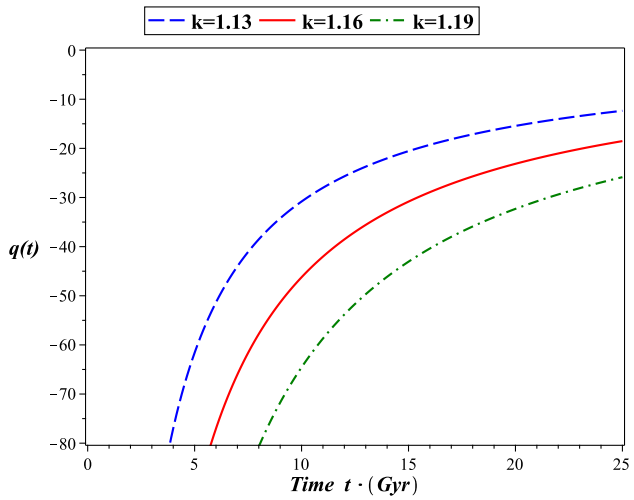

Fig. 8. Plot of the deceleration parameter q versus cosmic time t for $c_1 = -19000$.

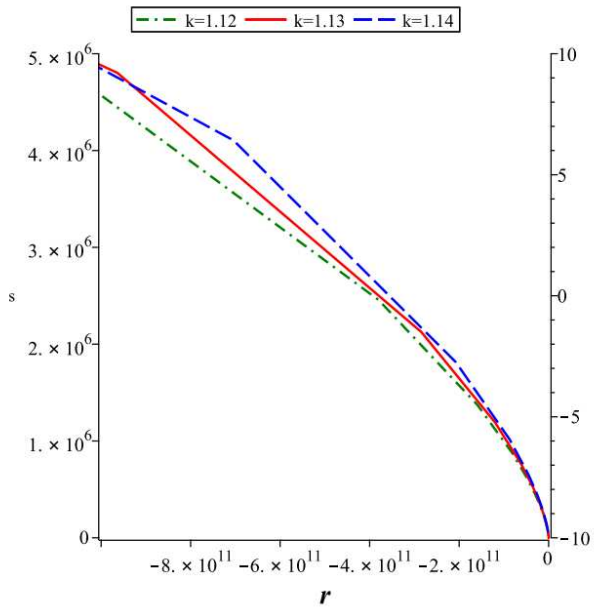

Fig. 9. Plot of the statefinder's plane for $c_1 = -19000$.

Energy conditions: For our dark energy, we go through the well-known energy conditions. The Raychaudhuri equations, which are central to any discussion of the congruence of null and time-like geodesics, gave rise to the study of energy conditions. The energy conditions are also used to demonstrate a va-

riety of general theorems about the behaviour of strong gravitational fields. The following are the typical energy conditions: dominant energy condition: $\rho_\Lambda \geq 0$, $\rho_\Lambda \pm p_\Lambda \geq 0$, weak energy conditions: $\rho_\Lambda \geq 0$, $\rho_\Lambda + p_\Lambda \geq 0$, null energy conditions: $\rho_\Lambda + p_\Lambda \geq 0$, strong energy conditions: $\rho_\Lambda + p_\Lambda \geq 0$, $\rho_\Lambda + 3p_\Lambda \geq 0$.

The energy conditions for our DE model are depicted in Figs. 2-4, where we have plotted them for various values of the parameters k and δ. It can be seen that the energy densities of matter and dark energy are decreasing functions of cosmic time t. But the energy density of matter does not exhibit any significant difference in behavior with change in the parameter δ. The null energy conditions are clearly violated, and the model results in a Big Rip. Also, as expected, our model violates the other energy conditions. This is due to the late-time acceleration of the universe, which is consistent with recent observational data.

EoS parameter: The EoS parameter is defined as the relationship between DE's pressure p_{de} and energy density ρ_{de}, which is expressed as $\omega_{de} = \frac{p_{de}}{\rho_{de}}$. The EoS parameter is used to classify the universe's decelerated and accelerated expansion, and it divides epochs into the following categories: for $\omega = 1$ (stiff fluid), $\omega = \frac{1}{3}$ (radiation), and $\omega = 0$ (matter dominated/dust) decelerating phases. It symbolizes the quintessence $-1 < \omega < -1/3$, the cosmological constant $\omega = -1$, and the phantom $\omega < -1$.

The EoS parameter of our DE model is depicted in Fig. 5 for various values of k and δ. We observe that the EoS parameter is behaving the same in both cases. It can be seen that the model starts in the matter dominated era and passes quintessence, cosmological constant, phantom, and attains a constant value in the aggressive phantom region ($\omega_{de} << -1$).

$\omega_{de} - \omega'_{de}$ plane: The dynamical property of dark energy models is studied using the $\omega_{de} - \omega'_{de}$ plane analysis, where prime ($\prime$) signifies derivative with regard to $ln(a(t))$. This method was suggested by Caldwell and Linder (2005) to analyse the behaviour of the quintessence model. They divided the $\omega_{de} - \omega'_{de}$ plane into thawing ($\omega_{de} < 0$ and $\omega'_{de} > 0$) and freezing ($\omega_{de} < 0$ and $\omega'_{de} < 0$) areas. Different researchers extended this planar analysis in a wide range for analysing the dynamical behaviour of various DE models and modified theories of gravity (Scherrer 2006; Chiba 2006; Sharif and Jawad 2013).

Our DE model's ω_{de}-ω'_{de} trajectory is depicted in Fig. 6 for different values of the parameter δ as the ω_{de}-ω'_{de} plane remains the same for various values of k. The model differs in the thawing and freezing regions, however the majority of the trajectory is in the freezing region. According to observational evidence, the expansion of the cosmos is significantly faster in the freezing area. As a result, the behaviour of the ω_{de}-ω'_{de} plane is consistent with current data.

Stability analysis: We use the squared speed of sound to assess the stability of our DE model in this scenario against small perturbations. The sign of v_s^2 plays an important role, as its negative ($v_s^2 < 0$) denotes instability and its

positive ($v_s^2 > 0$) shows stability. It is possible to define it as follows:

$$v_s^2 = \frac{\dot{p}_{de}}{\dot{\rho}_{de}}. \tag{34}$$

By differentiating the EoS parameter $\omega_{de} = \frac{p_{de}}{\rho_{de}}$ with regard to time t and dividing by $\dot{\rho}_{de}$, we get

$$v_s^2 = \omega_{de} + \frac{\rho_{de}}{\dot{\rho}_{de}}\ \dot{\omega}_{de}. \tag{35}$$

In the present scenario, we develop the squared speed of sound trajectories in terms of cosmic time as shown in Fig. 7 for different values of k and δ. We can observe from Fig. 7 that the v_s^2 curve exhibits negative behavior for both values of k and δ. Thus our model is unstable throughout the evolution of the universe. This behavior is quite similar to the DE model constructed by Maity and Debnath (2019).

Deceleration parameter: The deceleration parameter is an important kinematical quantity (q). This parameter indicates whether the universe is speeding up or slowing down. There is an accelerating expansion if $-1 < q < 0$, a decelerating expansion if $q > 0$, and a constant rate of expansion if $q = 0$. In addition, for $q = -1$, we get an exponential expansion and for $q < -1$, we have a super exponential expansion. The deceleration parameter obtained for our model is

$$q(t) = \frac{3\,t + 3\,c_1\ (k-1)^2}{(k+2)\,t} - 1. \tag{36}$$

In Fig. 8, we have plotted the deceleration parameter versus cosmic time for our model for various values of the parameter k. We see that the deceleration parameter remains less than -1 and eventually approaches -1 at late times for all values of k, indicating that the cosmos is accelerating. As a result, we have a universe that is expanding exponentially.

Statefinder parameters (r, s): Many different DE theories have been proposed to explain the universe's accelerating expansion. Sahni et al. (2003) have proposed statefinder parameters (r, s) to test the validity of these models. The $r-s$ plane is the cosmological plane corresponding to these parameters, and it indicates how far a certain DE model is from the ΛCDM limit. These parameters' cosmic planes characterize many well-known parts of the cosmos, e.g., $s > 0$ and $r < 1$ give the phantom and quintessence DE eras, respectively. $(r, s) = (1, 0)$ is the ΛCDM limit, $(r, s) = (1, 1)$ is the CDM limit, and $s < 0$ and $r > 1$ are the Chaplygin gas limits. Our models' statefinder parameters are provided by

$$r(t) = \frac{3\,t + 3\,c_1\ (k-1)^2}{(k+2)\,t} - 1 + 2\left(\frac{3\,t + 3\,c_1\ (k-1)^2}{(k+2)\,t} - 1\right)^2 + \frac{9c_1\ (k-1)^2\left(t^2 - c_1\ (k-1)^2\right)}{(k+2)^2\,t^3} \tag{37}$$

$$s(t) = \left\{ \frac{3\,t + 3\,c_1\,\,(k-1)^2}{(k+2)\,t} - 2 + 2\,\left(\frac{3\,t + 3\,c_1\,\,(k-1)^2}{(k+2)\,t} - 1 \right)^2 \right.$$
$$\left. +9\,\frac{c_1\,\,(k-1)^2\left(t^2 - c_1\,\,(k-1)^2\right)}{(k+2)^2\,t^3} \right\} \left(3\,\frac{3\,t + 3\,c_1\,\,(k-1)^2}{(k+2)\,t} - 4.5 \right)^{-1} \quad (38)$$

Plotting r versus s yields the statefinders plane, as shown in Fig. 9 for different values of k. The regions of quintessence and phantom models can be found in the $r-s$ plane for our model. This geometric behavior of our model is in quite good accordance with the EoS parameter behavior of our model.

Conclusions

In this paper, we present the Kantowski-Sachs universe with pressure-less matter and the Sharma-Mittal HDE in the context of the Brans-Dicke gravitational theory. Some physically plausible conditions are used to find the solution of field equations. By obtaining the cosmological parameters of our models, we can analyze the dynamical characteristics of our DE model. Some conclusions are as follows:

- Our model has no initial singularity and expands from a finite volume starting point. As $t \to \infty$, the physical parameters H, θ, σ^2 disappear and all drop to constant values at $t = 0$. Our model also becomes isotropic (because $A_h = 0$) and shear-free when $k = 1$. Our models' scalar field is positive and decreasing with cosmic time (Fig. 1). This behaviour is similar to that of scalar field models in several theories (Jawad et al. 2015; Aditya and Reddy 2019; Naidu et al. 2019; Raju et al. 2020b).
- We conclude that our model has a super exponential expansion (Fig. 8) based on the deceleration parameter. Several authors (Singh and Rani 2015; Naidu et al. 2019; Aditya and Reddy 2019; and Raju et al. 2020c) have reported similar findings. The trajectory of statefinder parameters changes in both quintessence and phantom regions (Fig. 9). The NEC is clearly violated, resulting in a Big Rip in the model. Our model also violates the other energy conditions, as expected. This is due to the universe's late-time acceleration, which is supported by new observational data.
- We plotted the squared speed of sound v_s^2 trajectory for our DE model in this scenario (Fig. 5). The model is unstable, which is demonstrated by the fact that v_s^2 varies fully in the negative region. The model starts in the matter-dominated era, crosses the phantom division line ($\omega_\Lambda = -1$), and finally reaches a constant value in the aggressive phantom region $\omega_\Lambda << -1$, according to the EoS parameter analysis. We investigated the $\omega_{de} - \omega'_{de}$ plane analysis and discovered that it occurs in both thawing and freezing phases of the universe (Fig. 5). The expansion of the cosmos is substantially faster in the freezing area, according to observational evidence. As a result, the $\omega_{de} - \omega'_{de}$ plane's behaviour is consistent with current data. Also, we have studied the behavior of all the dynamical parameters for different

values of k and δ. It is very clear from the figures that both the Brans-Dicke scalar field $\phi(t)$ (in view of constant k) and δ play a significant role in the dynamics of cosmological parameters.

Acknowledgments: The authors thank the anonymous referee whose valuable comments have helped in bringing the paper to the present form.

References

Aditya Y., et al. 2016, *Astrophys. Space Sci. 361, 56*
Aditya Y., Reddy, D.R.K., 2018, *Eur Phys J C. 78: 619.*
Aditya Y., et al., 2019a, *Eur. Phys. J. C 79, 1020.*
Aditya Y., et al., 2019b, *Astrophys Space Sci. 364, 190*
Aditya Y., Reddy, D.R.K., 2019, *Astrophys. Space Sci., 364, 3*
Aditya Y., et al., 2020, *Indian Journal of Phys. 95, 383-389*
Aditya Y., et al. 2021, *New Astronomy 84, 101504*
Aditya Y., et al. 2022, *International Journal of Modern Physics A 37(16), 2250107*
Bhaskara Rao M.P.V.V., et al., 2021, *International Journal of Modern Physics A, 36(36), 2150260*
Bhaskara Rao M.P.V.V., et al., 2022, *New Astronomy, 92, 101733*
Brans C., Dicke, R.H., 1961, *Phys. Rev. 124, 925*
Caldwell, R.R., 2002, *Phys. Lett. B 545, 23.*
Caldwell R., Linder E.V., 2005, *Phys Rev Lett 95, 141301.*
Chiba T., 2006, *Phys. Rev. D 73, 063501.*
Cohen A., Kaplan, D., Nelson, A., 1999, *Phys. Rev. Lett. 82, 4971.*
Collins C.B., et al. 1980, *Gen. Relativ. Gravit. 12: 805*
Dasunaidu K., et al., 2021, *Modern Physics Letters A 36, 2150054*
Divya Prasanthi U.Y., Aditya Y., 2020, *Results of Physics, 17, 103101.*
Divya Prasanthi U.Y., Aditya Y., 2021, *Physics of the Dark Universe, 31, 100782.*
Duran I., Pavon D., 2011, *Phys. Rev. D 83, 023504.*
Eriksen H.K., et al., 2004, *Astrophys. J., 605, 14-20.*
Gao Z.K., et al., 2006, *Phys. Rev. D 74, 127304.*
Ghaffari S., et al., 2019, *Physics of the Dark Universe 23, 100246.*
Ghaffari S., 2019, *New Astronomy 67, 76.*
Iqbal A., Jawad, A., 2019, *Physics of the Dark Universe 26, 100349.*
Jahromi A.S., et al., 2018, *Phys. Lett. B 780, 21.*
Jawad A., et al., 2015, *Commun. Theor.Phys. 64, 590.*
Jawad A., et al., 2018, *Symmetry 10, 635.*
Johri, VB, Sudharsan, R, 1989, *Australian Journal of Physics 42(2) 215 – 222.*
Johri VB, Desikan, K, 1994, *Gen RelatGravit 26, 1217–1232.*
Kantowski R., Sachs R.K.J., 1966, *Math Phys 7: 433.*
Li M., 2004, *Phys. Lett. B 603, 1.*
Maity S., Debnath U., 2019, *Eur. Phys. J. Plus 134, 514.*
Moradpour H., et al., 2018, *Eur. Phys. J. C 78, 829.*
Naidu K.D., et al. 2018, *Eur Phys J Plus. 133: 303*
Naidu R.L., et al., 2019, *Heliyon 5, e01645*
Naidu R.L., et al., 2020, *Astrophys Space Sci 365, 91*
Naidu R.L., et al. 2021, *New Astronomy 85, 101564*
Nojiri S., Odintsov S.D., 2006, *Gen. Rel. Grav. 38, 1285.*
Nojiri S., et al., 2019, *Phys. Lett. B 797, 134829.*
Padmanabhan T., 2008, *Gen. Relativ. Gravit. 40, 529.*
Perlmutter S., et al., 1999, *Astrophysical Journal, 517, 565-586.*
Raju K.D., et al. 2019, *Canadian Journal of Physics, 97, 932-937*
Raju K.D., et al., 2020a, *Astrophys. Space Sci. 365, 28.*
Raju K.D., et al., 2020b, *Astrophys. Space Sci. 365, 45*
Raju K.D., et al., 2020c, *Can. J. Phys. 98, 993*
Rao V.U.M., et al., 2015a, *Prespacetime J. 6, 531*
Rao V.U.M., et al., 2015b, *The African Review of Physics 10, 0060*
Rao V.U.M., et al., 2015c, *Prespacetime J. 6, 947*
Rao V.U.M., et al., 2018, *Results in Physics. 10: 469.*
Reddy D.R.K., et al., 2016, *Astrophys Space Sci. 361: 356*

Riess, A.G., et al., 1998, *Astron. J. 116, 1009–1038.*
Scherrer R.J., 2006, *Phys. Rev. D 73, 043502.*
Sharif M., Jawad A., 2013, *Eur. Phys. J. C 73, 2382.*
Sahni V., Starobinsky A.A., 2000, *Int. J. Mod. Phys. D 9, 373.*
Sahni V., et al., 2003, *Jetp Lett. 77, 201.*
Santhi M.V., et al., 2016, *Astrophys. Space Sci. 361, 142*
Santhi MV, et al., 2016, *Can. J. Phys., 94(6),578*
Santhi M.V., et al., 2017a, *Int. J. Theor. Phys. 56, 362.*
Santhi M.V., et al., 2017b, *Can J Phys. 95: 381-392*
Santhi M.V., et al. 2017c, *Int J Theor Phys. 56: 362.*
Santhi M.V., et al., 2017d, *Can. J. Phys., 95(2), 136*
Santhi M.V., et al., 2018, *Canadian Journal of Physics. Can. J. Phys. 96, 55*
Santhi M.V., et al., 2019, *Journal of Dynamical Systems & Geometric Theories 17, 23*
Sharif M., Zubair M., 2010, *Astrophys. Space Sci. 330, 399.*
Sharif M., Shamir M.F., 2010, *Gen Relativ Gravit, 42, 2643-2655*
Sharma U.K., Dubey V.C., 2020, *The European Physical Journal Plus, 135, 391.*
Sharma B.D., Mittal D.P. 1975, *J. Math. Sci. 10, 28.*
Singh J.K., Rani S., 2015, *Int J Theor Phys. 54: 545*
Susskind L., 1995, *J. Math. Phys. 36, 6377.*
Tanisman A.C., et al., 2019, *Eur. Phys. J. Plus 134, 325.*
Tavayef M., et al., 2018, *Phys. Lett. B. 781, 195.*
Thorne K.S., 1967, *Astrophysical Journal, 148, 51.*
Tsallis C., Cirto, L.J.L. 2013, *Eur. Phys. J. C 73, 2487.*
Wei H., Cai R.G., 2008, *Phys. Lett. B 660, 113.*
Xu L., Wang Y., 2010, *J. Cosmol. Astropart. Phys. 06, 002.*
Younas M., et al., 2019, *Advances in High Energy Physics 2019, 1287932.*